Journal of Materials Chemistry A

N-, Fe- and Co-Tridoped Carbon Nanotube/Nanoporous Carbon Nanocomposite with Synergistically Enhanced Activity for Oxygen Reduction in Acidic Media

Journal:	*Journal of Materials Chemistry A*
Manuscript ID:	TA-ART-05-2015-003523.R1
Article Type:	Paper
Date Submitted by the Author:	23-Jul-2015
Complete List of Authors:	Chen, Ping; Anhui University, School of Chemistry and Chemical engineering Wang, Gan; Anhui University, Wang, Wanhua; Anhui University, Wang, Li-Kun; Anhui University, Yao, Weitang; Southwest University of Science and Technology, Yao, Peng-Fei; Anhui University, Zhu, Wen-Kun; Southwest University of Science and Technology, Wu, Qingsheng; Tongji University, Department of Chemistry

Cite this: DOI: 10.1039/c0xx00000x

www.rsc.org/xxxxxx

ARTICLE TYPE

N-, Fe- and Co-Tridoped Carbon Nanotube/Nanoporous Carbon Nanocomposite with Synergistically Enhanced Activity for Oxygen Reduction in Acidic Media

Gan Wang [a,†], Wan-hua Wang [a,†], Li-Kun Wang [a,†], Wei-Tang Yao [b], Peng-Fei Yao [a], Wen-Kun Zhu [b], Ping Chen [a,*], Qing-Sheng Wu [c,*]

[a] School of Chemistry and Chemical Engineering, Anhui University, Hefei, Anhui, 230601, P. R. China; E-mail: chenping@ahu.edu.cn

[b] Joint Laboratory for Extreme Conditions Matter Properties, Southwest University of Science and Technology, Mianyang, Sichuan 621010, China

[c] Department of Chemistry; Key Laboratory of Yangtze River Water Environment, Ministry of Education, Tongji University, Shanghai 200092, P. R. China; E-mail: qswu@tongji.edu.cn; Tel: 021-65982620, Fax: 086-021-65981097

† These authors (Gan Wang a,†, Wanhua Wang a,†, Li-Kun Wang a,†) have the equal contribution to this paper.

Electronic supplementary information (ESI) available

Received (in XXX, XXX) Xth XXXXXXXXX 20XX, Accepted Xth XXXXXXXXX 20XX

DOI: 10.1039/b000000x

Abstract: Electrocatalyst for oxygen reduction reaction (ORR) in acidic media is crucial in proton-exchange membrane (PEM) fuel cells and other electrochemical devices. Achieving ideal ORR activity and durability in acidic media remains a challenge. **Here**, we developed a new NFeCo-CNT/NC nanocomposite electrocatalyst from the highly available and recyclable plant biomass *Typha orientalis* using a readily scalable approach. The electrocatalyst exhibits the excellent ORR activity, superior stability and tolerance to methanol poisoning effects in the acidic media. The value of onset potential and half-peak potential of the typical product is only 70 mV and 65 mV less than that of the Pt/C, respectively. The NFeCo-CNT and NFeCo-NC in the nanocomposite have the synergistically enhanced ORR activities. The catalyst may have practical applications in fuel cells. One of the important accomplishments of this work is the discovery that trace Fe^{3+} and Co^{2+} can synergistically catalyze the growth of the carbon nanotube when melamine serve as CNT precursor.

1. Introduction

Electrocatalyst for oxygen reduction reaction (ORR) in acidic media is crucial in proton-exchange membrane (PEM) fuel cells and other electrochemical devices.[1-4] Replacing precious and nondurable Pt catalysts with cheap and commercially available materials for ORR is still a key issue in the development of material science and fuel cell technology.[5-8] So far, great efforts have been devoted to prepare the heteroatom (e.g., N, P, B and S)-

doped nanostructured carbon materials, which exhibit an ORR performance comparable to that of commercial Pt/C in alkaline media. Especially, many researches focus on the doping of nitrogen in the carbon, because it can remarkably promote the catalytical ability, improve the stability and tolerance to methanol poisoning effects of the ORR catalysts.[9-17] It is well-known that PEM fuel cells can only be worked with acidic electrolytes.[3, 4] Unfortunately, the carbon materials exhibit the dissatisfactory or even very weak ORR performance in acidic media.

Some researches show the addition of certain transition metals (e.g., Fe, Co) to the nitrogen-doped carbon materials can promote the ORR activity in acidic media. The transition-metal cation can coordinate with the nitrogen doped in the carbon materials.[7, 18] Careful selection of suitable nitrogen/transition-metal precursors and carbon supports can achieve the obviously improved ORR activity.[19-21] However, obtaining the catalysts with comparable activity and durability with the state-of-the-art Pt/C remains a challenging work. In principle and fact, in order to improve the ORR activity, nanoscale porosity is highly desirable, which can facilitate high mass transfer fluxes and high active loading.[22-24] Especially, micropores are crucial for good catalysts.[25, 26] For the purpose of the practical application in the fuel cells, the ORR catalysts should be low-cost, high-volume production.[15, 27, 28] The catalysts directly derived from biomass are ideal because biomass is an environmentally friendly and recyclable resource and often is highly available, accessible and low-cost.[23, 29, 30]

Recently, we reported a kind of nitrogen-doped nanoprous carbon nanosheets from the highly available, accessible and recyclable plant *Typha orientalis*. In alkaline media, the material exhibits similar catalytic activity but superior tolerance to methanol to 20 % Pt/C.[31] We also developed the nitrogen-doped graphene/carbon nanotube nanocomposite by a facile hydrothermal process at a low temperature, and the typical product exhibits the synergistically enhanced ORR activity in alkaline media.[32] **Herein,** we prepared a new N-, Fe- and Co-tridoped carbon nanotube/nanoporous carbon (NFeCo-CNT/NC) nanocomposite from the plant biomass *Typha orientalis* using a readily scalable approach. The product exhibits the excellent ORR activity, superior stability and tolerance to methanol poisoning effects in the acidic media. The NFeCo-CNT and NFeCo-NC in the nanocomposite can synergistically enhance the ORR activities. Very importantly, we found that trace Fe^{3+} and Co^{2+} can synergistically catalyze the growth of the carbon nanotube when melamine serve as CNT precursor.

2. Experimental section

2.1 Chemicals

All reagents are of analytical grade and used without further purification. KOH, $FeCl_3$, HCl and $C_4H_6CoO_4{\cdot}4H_2O$ were purchased from Aladdin industrial corporation (Shanghai, P.R. China). NH_3 (99.9 %) was purchased from Yang Yuan Company (Nanjing). *Typha orientalis* was obtained from a local wetland, washed by distilled water and crushed.

2.2 Preparation

Preparation of Nanoporous Carbon (NC). Typically, 6.0 g flower spikes of *Typha orientalis* were split and put into an autoclave with a volume of 100 mL. After the hydrothermal process at 180 °C for 10 h, the black carbonaceous hydrogel was obtained. After washing with distilled water for several times, the carbonaceous aerogel was obtained by freeze drying for 12 h. 4.8 g KOH, 4g carbonaceous aerogel and 20 mL distilled water were mixed and placed for 12 h. Then, the dried mixture was obtained by freeze drying for 12 h and annealed in N_2 atmosphere at 850 °C for 1 h with the heating rate of 5 °C/min and the cooling rate of 5 °C/min. Finally, the nanoporous carbon was obtained after 10 % HCl treatment.

Preparation of N-, Fe- and Co-Tridoped Carbon Nanotube/ Nanoporous Carbon Nanocomposite (NFeCo-CNT/NC). Typically, 100.0 mg of the above nanoporous carbon was dispersed in the 10 mL distilled water. 3.0 mg $FeCl_3$ and 2.0 mg $C_4H_6CoO_4{\cdot}4H_2O$ were added to the mixture solution, which was stirred magnetically at 25 ^oC for 40 min. The dried mixture was obtained by freeze drying for 10 h. Then, 500 mg melamine was added to the dried mixture by grind process and the dried mixture was annealed in N_2 atmosphere at 900 °C for 1 h with the heating rate of 5 °C/min and the cooling rate of 5 °C/min. Finally the typical NFeCo-CNT/NC was obtained.

For comparison, we prepared the Fe- and Co-doped nanoporous carbon (FeCo-NC) according to the same steps as typical NFeCo-CNT/NC catalyst but without melamine. We also prepared the N-, Fe- and Co-tridoped carbon nanotube (NFeCo-CNT) according to the same steps as typical NFeCo-CNT/NC catalyst but without nanoporous carbon.

2.3 Characterization

Scanning electron microscopy (SEM) images were obtained on a field emission scanning electron microanalyzer (JEOL-6700F). SEM samples were prepared by drop-drying the samples onto silicon substrates. Scanning Transmission electron microscopy (STEM) images were recorded on a JEM-2100F with an EDX analytical system. STEM samples were prepared by drop-drying the samples onto copper grids. X-ray photoelectron spectroscopic (XPS) data were achieved on an X-ray photoelectron spectrometer (ESCALab MKII). BET surface areas were obtained on a Micrometrics ASAP2020 analyzer (USA). X-ray diffraction patterns (XRD) of the products were performed on an XD-3 X-ray diffractometer. Raman spectra were taken by an inVia-Reflex spectrometer (Renishaw) with a 532 nm laser excitation.

2.4 Electrochemical measurements

CHI 730E electrochemical workstation (Shanghai Chenhua, China) was used to measure the electrochemical activities of the samples in a three-electrode cell at room temperature. ORR activities of the samples were investigated by rotating disk electrode (RDE) and rotating ring-disk electrode (RRDE). A glassy carbon disk (GC, PINE, 5 mm diameter, 0.196 cm^2) was used as the working electrode. Ag/AgCl was used as reference electrode and platinum plate was used as counter electrode. The working electrode was scanned at a rate of 20 mVs^{-1} with the rotating speed from 400 rpm to 2000 rpm in O_2-saturated 0.5 M H_2SO_4. For each sample (including 20 % Pt/C catalyst), 5 mg of catalyst powder was dispersed in 1mL of 3:1 v/v DIW/isopropanol mixed solvent with 40 uL Nafion solution (5 wt %). Then, the mixture was ultrasonicated for 30 min to obtain the catalyst ink.[11] Next, 8 uL of the ink was transferred and adhered on the GC disk electrode (catalyst loading of 0.200 mg/cm^2).

In the RRDE measurements, catalyst and electrodes were prepared by the same method as above. The ring current (I_R) was measured with a Pt ring electrode in the 0.5 M H_2SO_4. Pt ring electrode was polarized at 0.955 V (vs RHE). The four-electron selectivity of the catalyst was evaluated based on the H_2O_2 yield. The H_2O_2 yield and the electron transfer number (n) were determined by the following equations:[11]

$$\%(H_2O_2) = 200 \times \frac{I_R / N}{I_D + I_R / N} \quad (1)$$

$$n = 4 \times \frac{I_D}{I_D + I_R / N} \quad (2)$$

where I_D is the disk current, and I_R is the ring current, and N is current collection efficiency of the Pt ring. N is 0.35 from the reduction of $K_3Fe[CN]_6$.[31]

The calibration of Ag/AgCl electrode was performed in a standard three-electrode system with polished Pt wires as the working and counter electrodes, and the Ag/AgCl electrode as the reference

electrode. Electrolytes are pre-purged and saturated with high purity H_2. In 0.5 M H_2SO_4, E (RHE) = E (Ag/AgCl) + 0.23 V.[31]

3. Results and discussion

3.1 Preparation

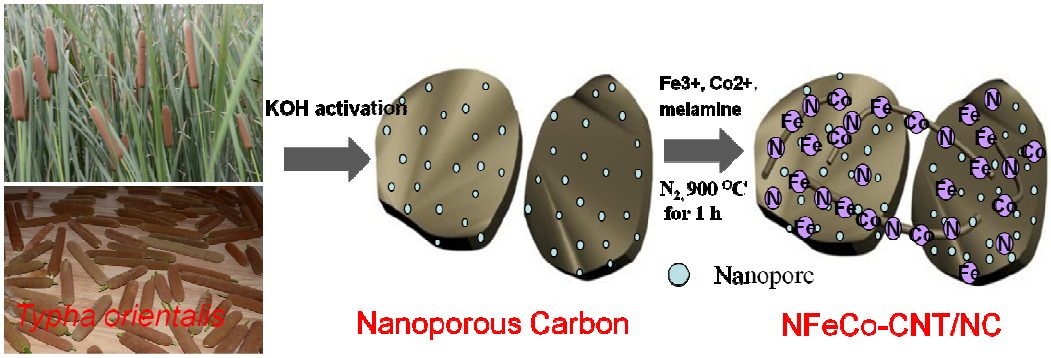

Scheme 1. Illustration of the preparation of the typical NFeCo-CNT/NC

Scheme 1 showed the illustration of the proposed formation of the typical NFeCo-CNT/NC. Firstly, *Typha orientalis* was obtained from a local wetland, washed with distilled water and crushed. Flower spikes of *Typha orientalis* were split and put into an autoclave. After the hydrothermal process and freeze drying, the carbonaceous aerogel was obtained.[31] After KOH activation, the nanoporous carbon (NC) was obtained from the aerogel. (SEM images, high-resolution C1s XPS spectra and nitrogen adsorption-desorption isotherm of the NC were shown in the Fig. S1, see the ESI†) Then, 100.0 mg of the NC was dispersed in the distilled water. 3.0 mg ferric trichloride ($FeCl_3$) and 2.0 mg cobalt (II) acetate ($C_4H_6CoO_4{\cdot}4H_2O$) were added to the mixture solution, which was stirred magnetically. The dried mixture was obtained by freeze drying for 10 h. Then, melamine was added to the dried mixture by grind process. Finally, the dried mixture was annealed in N_2 atmosphere at 900 °C for 1 h and the typical NFeCo-CNT/NC was obtained. In the annealing, the trace Fe^{3+} and Co^{2+} can synergistically catalyze the growth of the carbon nanotube from the melamine. The N element doped in the product was from melamine. We can adjust the ratio of $FeCl_3$ and $C_4H_6CoO_4.4H_2O$ content to obtain the products with different content of carbon nanotube. When the ratio of $FeCl_3$ to $C_4H_6CoO_4{\cdot}4H_2O$ content is 3/2, the product has more carbon nanotubes than others.

3.2 Characterization

The scanning electron microscopy (SEM, Fig. 1a) and the scanning transmission electron microscopy (STEM, Fig. 1b-c) clearly revealed the typical NFeCo-CNT/NC including carbon particles and nanotubes with the diameter from 35 to 45 nm. The elemental mappings (Fig. 1d-h) and elemental analysis image (Fig. 1i) indicate the presence of carbon, nitrogen, oxygen, ferrum and cobalt elements, which were homogeneously dispersed in the sproduct. Fig. S2a and Fig. S3a (see the ESI†) shows the STEM images of the typical NFeCo-CNT/NC in the square region marked with A and B in the Fig. 1b, respectively. Fig. S1b-f and Fig. S2b-f show carbon, nitrogen, oxygen, ferrum and cobalt element mappings in the square region marked with A and B in the Fig. 1b, respectively. Fig. S1g-h and Fig. S2g-h exhibits the elemental analysis data in the square region marked with A and B in the Fig. 1b, respectively. The product in the square region marked with A and B was doped by the nitrogen, ferrum and cobalt elements, respectively. However, the square region marked

with A contains higher nitrogen, ferrum and cobalt content than the square region marked with B.

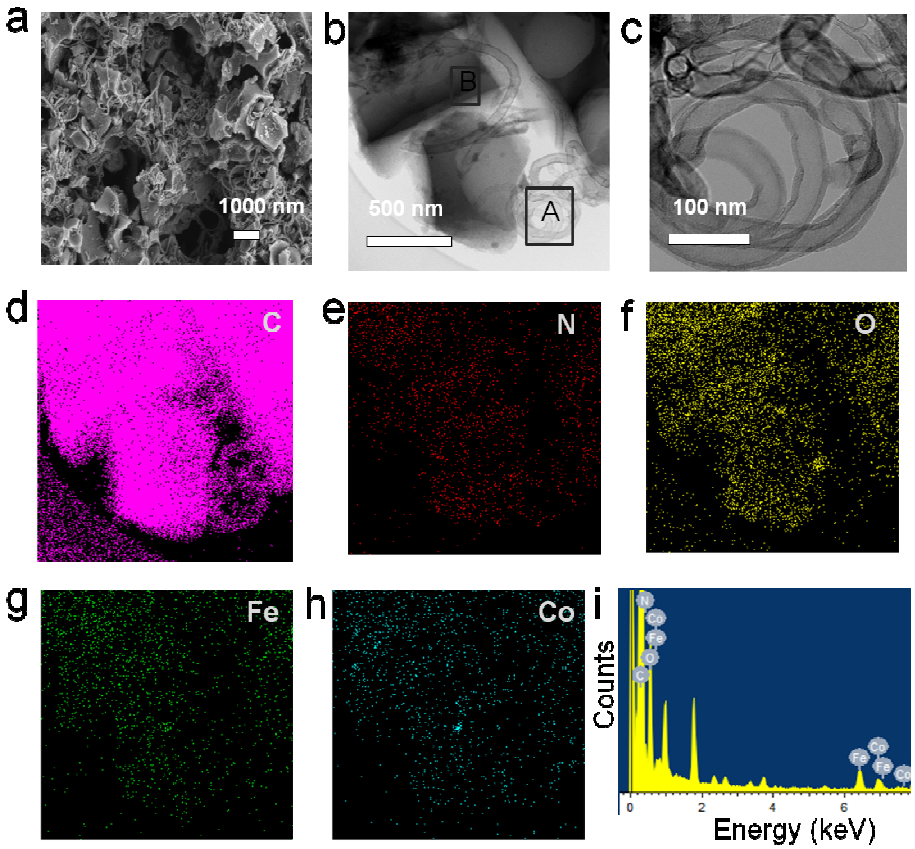

Fig. 1. (a-b) SEM and STEM images of the typical NFeCo-CNT/NC; (c) STEM image of the typical NFeCo-CNT/NC in the square region marked with **A** in the Fig. 1b; (d-h) carbon, nitrogen, oxygen, ferrum and cobalt element mappings; (i) elemental analysis image of the typical NFeCo-CNT/NC

The data of the X-ray photoelectron spectroscopy (XPS) were shown in the Fig. 2a-d. For the high resolution of C1s spectra, the peak at 284.8 eV corresponds to the sp^2-hybridized graphitic carbon, the peaks at 286.1 eV and 288.1 eV are attributed to C-OH and C=O configurations, respectively.[32, 33] Fig. 2b indicates mainly four kinds of nitrogen were doped. The peak at 398.5 eV can be ascribed to pyridinic N species, and the peak at 399.5 eV corresponds to amine moieties or other sp^3-C and nitrogen bonds. The peak at 400.4 eV can be ascribed to pyrrolic structure, and the peak at 401.1 eV corresponds to the graphitic N.[32] From the Fig. 2c, the peaks at 713.2 eV are ascribed to the Fe^{2+} $2p_{3/2}$.[34] From the Fig. 2d, the peaks at 781.2 eV are ascribed to the Co^{2+} $2p_{3/2}$. According to the XPS data (see the ESI†, Table S1), 3.28 at.% of the N, 0.36 at.% of the Fe and 0.28 at.% of the Co were doped in the typical product. Fig. S4a (see the ESI†) indicates the amorphous nature of carbon for the product. Raman spectra (Fig. S4b) show that the typical product exhibits the remarkable peaks at around 1335 and 1588 cm^{-1} corresponding to the D band and G band, respectively. Fig. 2e and f show the N_2 adsorption-desorption isotherms and micropore size distribution. The BET surface area, total pore volume and micropore volume of the typical product was 866.00 m^2 g^{-1}, 0.50 cm^3 g^{-1} and 0.33 cm^3 g^{-1}, respectively. The micropore size distribution becomes around 0.54 nm.

Cite this: DOI: 10.1039/c0xx00000x

www.rsc.org/xxxxxx

ARTICLE TYPE

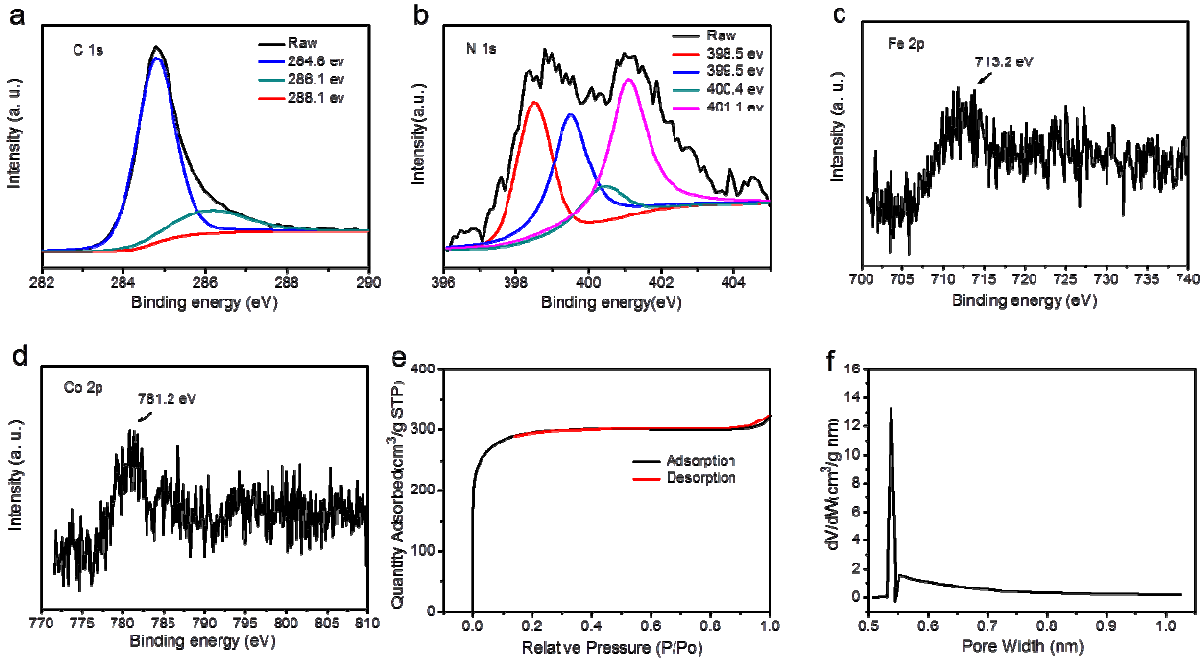

Fig. 2. (a-d) The high-resolution C1s, N1s, Fe2p and Co2p XPS spectra of the typical NFeCo-CNT/NC; (e-f) Nitrogen adsorption-desorption isotherm and micropore size distribution (slit pore geometry) of the typical NFeCo-CNT/NC.

3.3 Electrocatalytic activities

Rotating disk electrode (RDE) and rotating ring-disk electrode (RRDE) measurements were performed to investigate the ORR activities. We tested the ORR activities in the acidic media (0.5 M H_2SO_4). For comparison, commercial 20 wt % platinum on carbon black (Pt/C) (Johnson Matthey) was also measured. The results were shown in the Fig. 3. For the typical NFeCo-CNT/NC and commercial Pt/C, the value of onset potential was 840 and 910 mV (vs RHE), respectively (Fig. 3a). The value of onset potential and half-peak potential of the typical product is only 70 mV and 65 mV less than that of the Pt/C, respectively. Remarkably, when the potential is lowe than 640 mV (vs RHE), the current density of the product electrode is larger than that of commercial Pt/C. According to the reported literature, the typical NFeCo-CNT/NC exhibits the excellent ORR activity in acidic media. So far, achieving ideal ORR activity and durability in acidic media remains a challenge.[5, 19, 21, 34, 35] Compared with the previous work (nitrogen-doped nanoporous carbon nanosheets derived from the Typha orientalis), the typical NFeCo-CNT/NC shows the obviously improved onset potential, half-peak and reduction current in the acidic media.[31] RDE voltammograms for the ORR on the typical product and Pt/C electrode at the various rotation speeds were shown in the Fig. S5a and b (see the ESI†), respectively. We measured the possible poisoning effects of the typical NFeCo-CNT/NC and Pt/C in O_2-saturated 0.5 M H_2SO_4 with 1.0 M methanol. The results were shown in the Fig. 3b and c. Compared to Pt/C, the typical NFeCo-CNT/NC shows little activity loss, which indicates that the typical product has excellent tolerance to methanol poisoning effects. Fig. 3d shows the current-time (i-t) chronoamperometric response of the typical

NFeCo-CNT/NC and Pt/C electrodes. After 20000 seconds, the Pt/C suffered from a 32.0 % decrease in current density while the typical product showed the 27.0 % loss of current density, which indicates the typical product has a better durability than the Pt/C. Fig. 3e shows the RRDE voltammograms for the typical product, from which the peroxide yield and electron transfer number were obtained (Fig. 3f). The peroxide yield remained below 3.2 % at the potentials from 0.1 -1.0 V (versus RHE) and electron transfer number was calculated to be 3.95-4.00, which reveals an intrinsic four-electron-transfer process.

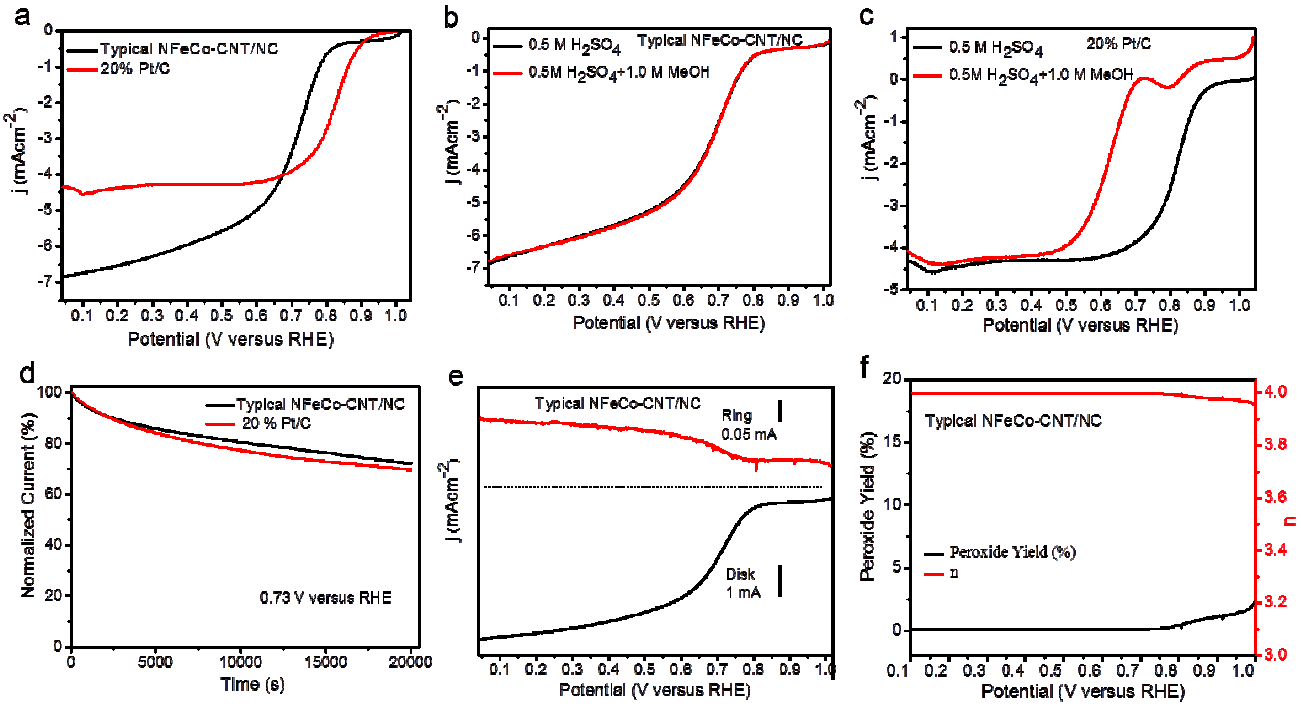

Fig. 3. (a) RDE voltammograms in O_2-saturated 0.5 M H_2SO_4 at room temperature (rotation speed 1600 rpm, sweep rate 20 mV s^{-1}) for the typical NFeCo-CNT/NC and Pt/C; (b) RDE voltammograms for the typical NFeCo-CNT/NC with or without 1.0 M methanol; (c) RDE voltammograms for the Pt/C with or without 1.0 M methanol; (d) Current-time (i-t) chronoamperometric response of the typical NFeCo-CNT/NC and Pt/C electrodes at 0.730 V (versus RHE) at a rotation rate of 800 rpm; (e-f) RRDE voltammograms, the electron transfer number (n) and peroxide yield for the typical NFeCo-CNT/NC in O_2-saturated 0.5 M H_2SO_4.

For comparison, we prepared the FeCo-NC according to the same steps as typical NFeCo-CNT/NC catalyst but without melamine and the NFeCo-CNT according to the same steps as typical NFeCo-CNT/NC catalyst but without nanoporous carbon. Fig. 4a-b show the FeCo-NC contains carbon particles without nanotubes and the NFeCo-NCNT mainly contains carbon nanotubes with the diameter from 60 to 90 nm. Nitrogen adsorption-desorption isotherms of the FeCo-NC and NFeCo-CNT were shown in the Figure S6. The BET surface area of the FeCo-NC and NFeCo-CNT was 1606.00 and 73.84 m^2 g^{-1}, respectively. Content of C, N, O, Fe and Co of the FeCo-NC and NFeCo-NCNT from the XPS data were shown in Table S1**.** Fig. 4c shows RDE voltammograms in O_2-saturated 0.5 M H_2SO_4 for the typical NFeCo-CNT/NC, NC, FeCo-NC and NFeCo-NCNT. Compared to the FeCo-NC, NFeCo-NCNT and NC, the typical NFeCo-CNT/NC shows the remarkably higher onset potential, half-peak potential and reduction current. Electrochemical impedance spectroscopy (EIS) was used to test the charge transfer resistance at the electrode surface and describe the interface properties.[32, 36] Fig. 4d shows the impedance data in N_2-saturated 0.5 M H_2SO_4.

Nyquist plots of typical NFeCo-CNT/NC exhibit the obviuosly small charge transfer resistance as compared with FeCo-NC, NFeCo-NCNT and NC. Therefore, the typical NFeCo-CNT/NC is the most effective in shuttling charges from electrode to solution, and the ORR activity can be remarkably promoted.

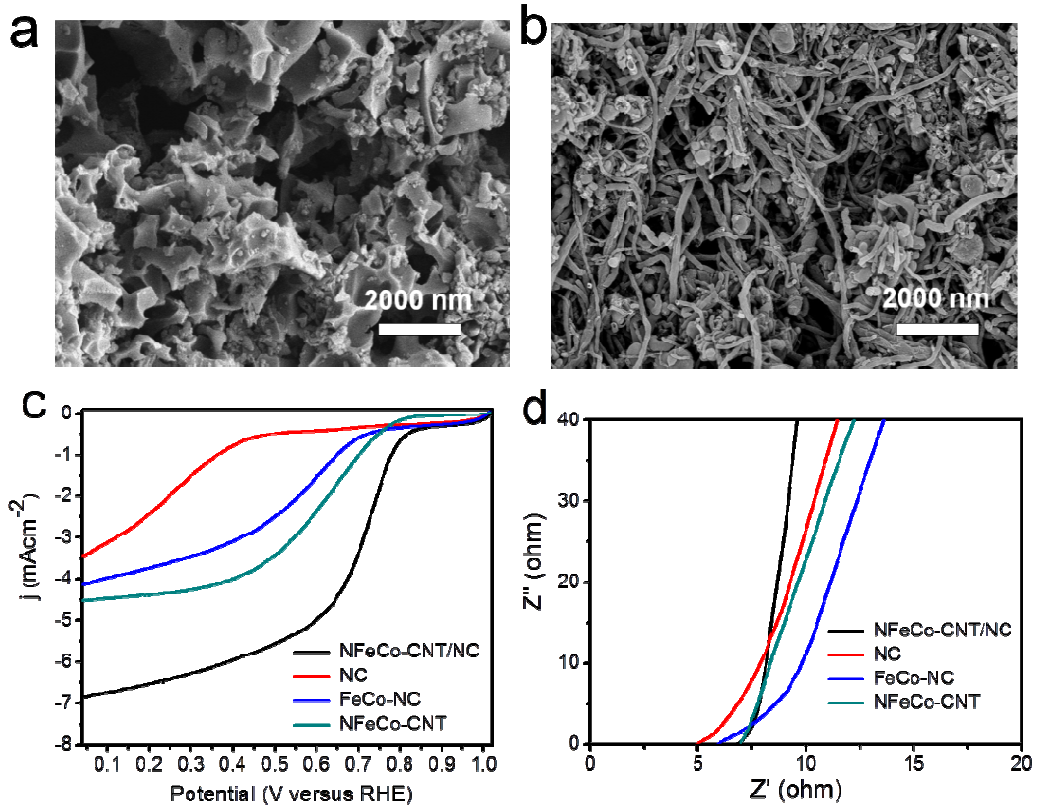

Fig. 4. (a-b) SEM images of the FeCo-NC and NFeCo-NCNT; (c) RDE voltammograms in O_2-saturated 0.5 M H_2SO_4 at room temperature (rotation speed 1600 rpm, sweep rate 20 mVs^{-1}) for the typical NFeCo-CNT/NC, NC, FeCo-NC and NFeCo-NCNT; (d) Impedance data of the typical NFeCo-CNT/NC, NC, FeCo-NC and NFeCo-NCNT in N_2-saturated 0.5 M H_2SO_4.

We investigate the effect of Fe and Co content on the ORR activity. Fig. 5 shows the SEM images of the NFeCo-CNT/NC with the different ratio of $FeCl_3$ to $C_4H_6CoO_4{\cdot}4H_2O$ content (w/w) in the preparation. From the Fig. 5, controlling the appropriate ratio of Fe to Co content is crucial in the produce of the carbon nanotube. When the ratio of $FeCl_3$ to $C_4H_6CoO_4{\cdot}4H_2O$ content is 3/2, the product has more carbon nanotubes than others. The effect of ratio of Fe and Co content on the ORR activity was shown in the Fig. 6a, from which the Fe and Co content can obviously affect the onset potential, half-peak potential and reduction current. By controlling the appropriate ratio, the onset potential, half-peak potential and reduction current can be remarkably promoted. We can obtain the product with best performance when the ratio of $FeCl_3$ to $C_4H_6CoO_4.4H_2O$ content is 3/2. The optimal product contains more carbon nanotubes than the others. Fig. S7a-d show the SEM images of the products using different amount of $FeCl_3$ without $C_4H_6CoO_4{\cdot}4H_2O$. Only when 33 mg $FeCl_3$ (without $C_4H_6CoO_4{\cdot}4H_2O$) were added in the preparation, the nanotube can be produced. From the Fig. S6e, when $C_4H_6CoO_4 4H_2O$ (without $FeCl_3$) was added in the preparation, the nanotube can not be produced. Therefore, we found that trace Fe^{3+} and Co^{2+} can synergistically catalyze the

growth of the carbon nanotube in the nanoporous carbon when the melamine serve as CNT precursor.

The effect of annealing temperature, annealing time and amount of the melamine on the ORR activity was measured (Fig. 6b-d). From the Fig. 6b-c, the optimal annealing temperature and time is 900 ^{o}C and 60 min. From the Fig. 6d, the optimal amount of the melamine is 500 mg in the preparation.

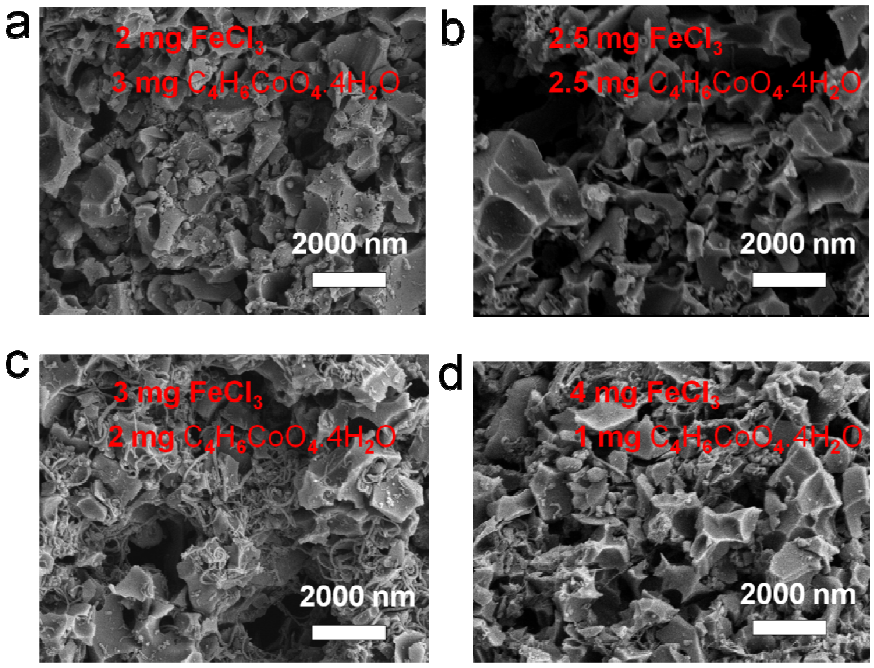

Fig. 5. (a-d) SEM images of the NFeCo(2/3)-CNT/NC, NFeCo(2.5/2.5)-CNT/NC, NFeCo(3/2)-CNT/NC and NFeCo(4/1)-CNT/NC

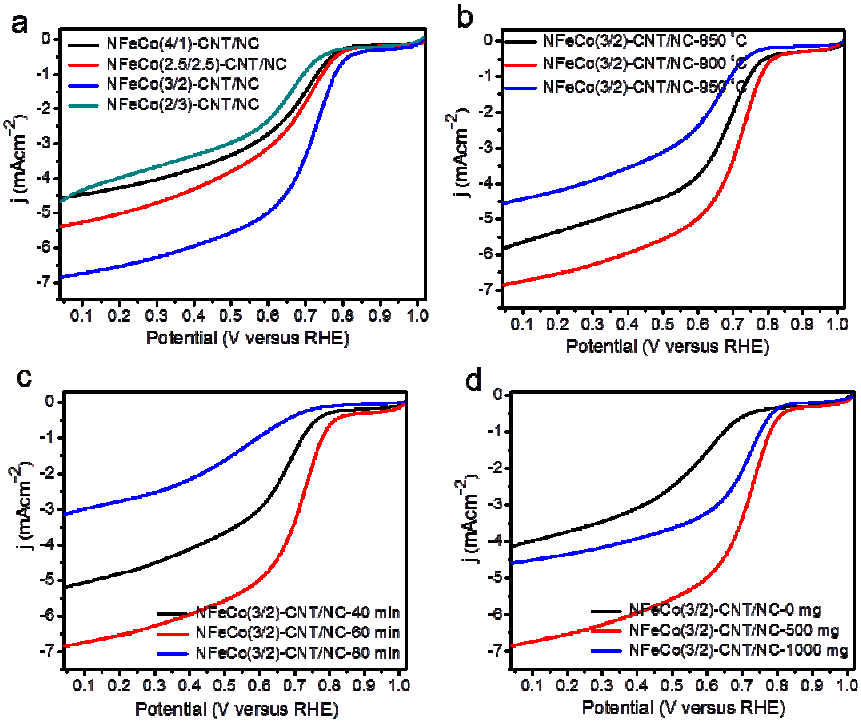

Fig. 6. (a) The effect of Fe and Co content on the ORR activity; (b) The effect of annealing temperature on the ORR activity; (c) The effect of annealing time on the ORR activity; (f) The effect of amount of the melamine on the ORR activity.

Cite this: DOI: 10.1039/c0xx00000x

www.rsc.org/xxxxxx

ARTICLE TYPE

From the above discussion, different ratio of carbon particles (NFeCo-NC) and nanotubes (NFeCo-CNT) in the product has an important role in the ORR activity. By controlling the appropriate ratio, the onset potential, half-peak potential and reduction current can be remarkably promoted. These results further prove that the NFeCo-NC and NFeCo-CNT in the NFeCo-CNT/NC have the synergistically enhanced ORR activities. There are probably three crucial reasons for the promoted ORR activity. Firstly, the N, Fe and Co elements doped within the carbon materials can enhance the ORR activity. The product contains the pyridinic N and graphitic N, which are the main components indicating the high ORR activity.[32] Research shows the trace Fe and Co elements doped within the carbon materials can obviously promote the ORR activity.[14, 20, 34, 37] Secondly, the typical NFeCo-CNT/NC has the high BET surface are (866.00 $m^2 g^{-1}$), total pore volume (0.50 $cm^3 g^{-1}$) and micropore volume (0.33 $cm^3 g^{-1}$), which can provide more active sites and facilitate high mass transfer fluxes.[25, 31] Thirdly, combining the NFeCo-NC with NFeCo-NCNT will produce a three dimension interpenetrated network structure, which effectively accelerates reactant, ion and electron transport.[32, 38,39]

4. Conclusions

In summary, we developed a new NFeCo-CNT/NC nanocomposite electrocatalyst from the highly available and recyclable plant biomass *Typha orientalis* using a readily scalable approach. The electrocatalyst exhibits the excellent ORR activity, superior stability and tolerance to methanol poisoning effects in the acidic media. The NFeCo-CNT and NFeCo-NC in the nanocomposite have the synergistically enhanced ORR activities. The catalyst promises to have practical applications in fuel cells. One of the important accomplishments of this work is the discovery that trace Fe^{3+} and Co^{2+} can synergistically catalyze the growth of the carbon nanotube in the nanoporous carbon when melamine serve as CNT precursor.

Acknowledgements

We acknowledge the funding support from the National Natural Science Foundation of China (Grants 21271005, 91122025, 21471114), the State Major Research Plan (973) of China (No. 2011CB932404), Project of Anhui University (02303203-0054) and the College Students' Innovation and Entrepreneurship Training Project (J18515020).

Notes and references

1 R. Borup, J. Meyers, B. Pivovar,Y. S. Kim, R. Mukundan, N. Garland, et al Chem. Rev., 2007, 107, 3904.

2 F. Charreteur, F. Jaouen, S. Ruggeri, J. P. Dodelet, Electrochim. Acta, 2008, 53, 2925.

3 H. A. Gasteiger, J. E. Panels, S. G. Yan, J. Power Sources, 2004, 127, 162.

4 X. X. Yuan, X. Zeng, H. J. Zhang, Z. F. Ma, C. Y. Wang, J. Am. Chem. Soc., 2010, 132, 1754.

5 G. Wu, P. Zelenay, *Acc. Chem. Res.*, 2013, **46**, 1878.

6 C. Sealy, *Mater Today*, 2008, **11**, 65.

7 G. Wu, K. L. More, C. M. Johnston, P. Zelenay, *Science*, 2011, **332**, 443.

8 Y. H. Bing, H. S. Liu, L. Zhang, D. Ghosh, J. J. Zhang, *Chem. Soc. Rev.*, 2010, **39**, 2184.

9 K. P. Gong, F. Du, Z. H. Xia, M. Durstock, L. M. Dai, *Science*, 2009, **323**, 760.

10 R. Cao, R. Thapa, H. Kim, X. Xu, M. G. Kim, Q. Li, N. Park, M. L. Liu, J. Cho, *Nat. Commun.*, 2013, **4**.

11 Y. Y. Liang, Y. G. Li, H. L. Wang, J. G. Zhou, J. Wang, T. Regier, H. J. Dai, *Nat. Mater.*, 2011, **10**, 780.

12 Y. G. Li, M. Gong, Y. Y. Liang, J. Feng, J. E. Kim, H. L. Wang, G. S. Hong, B. Zhang, H. J. Dai, *Nat. Commun.*, 2013, **4**.

13 H. T. Chung, J. H. Won, P. Zelenay, *Nat. Commun.*, 2013, **4**.

14 J. Liu, X. J. Sun, P. Song, Y. W. Zhang, W. Xing, W. L. Xu, *Adv. Mater.*, 2013, **25**, 6879.

15 M. M. Liu, R. Z. Zhang, W. Chen, *Chem. Rev.*, 2014, **114**, 5117.

16 Z. Schnepp, Y. J. Zhang, M. J. Hollamby, B. R. Pauw, M. Tanaka, Y. Matsushita, Y. Sakka, *J. Mater. Chem. A* ,2013, **1**, 13576.

17 H. Shi, Y. F. Shen, F. He, Y. Li, A. R. Liu, S. Q. Liu, Y. J. Zhang, *J. Mater. Chem. A,* 2014, **2**, 15704.

18 F. Jaouen, E. Proietti, M. Lefevre, R. Chenitz, J. P. Dodelet, G. Wu, H. T. Chung, C. M. Johnston,P. Zelenay, *Energy Environ. Sci.*, 2011, **4**, 114.

19 H. W. Liang, W. Wei, Z. S. Wu, X. L. Feng, K. Mullen, *J. Am. Chem. Soc.*, 2013, **135**, 16002.

20 L. Lin, Q. Zhu, A. W. Xu, *J. Am. Chem. Soc.*, 2014, **136**, 11027.

21 W. X. Yang, X. J. Liu, X. Y. Yue, J. B. Jia, S. J. Guo, *J. Am. Chem. Soc.*, 2015, **137**, 1436.

22 M. K. Debe, *Nature*, 2012, **486**, 43.

23 M. M. Titirici, R. J. White, C. Falco, M. Sevilla, *Energy Environ. Sci.*, 2012, **5**, 6796.

24 J. Liang, R. F. Zhou, X. M. Chen, Y. H. Tang, S. Z. Qiao, *Adv. Mater.*, 2014, **26**, 6074.

25 F. Jaouen, M. Lefevre, J. P. Dodelet, M. Cai, *J. Phys. Chem. B*, 2006, **110**, 5553.

26 F. Jaouen, F. Charreteur, J. P. Dodelet, *J. Electrochem. Soc.*, 2006, **153**, A689.

27 R. Bashyam, P. Zelenay, *Nature*, 2006, **443**, 63.

28 M. Lefevre, J. P. Dodelet, *Ecs. Transactions*, 2012, **45**, 35.

29 B. Hu, K. Wang, L. H. Wu, S. H. Yu, M. Antonietti, M. M. Titirici, *Adv. Mater.*, 2010, **22**, 813.

30 M. M. Titirici, A. Thomas, S. H. Yu, J. O. Muller, M. Antonietti, *Chem. Mater.*, 2007, **19**, 4205.

31 P. Chen, L. K. Wang, G. Wang, M. R. Gao, J. Ge, W. J. Yuan, Y. H. Shen, A. J. Xie, S. H. Yu, *Energy Environ. Sci.*, 2014, **7**, 4095.

32 P. Chen, T. Y. Xiao, Y. H. Qian, S. S. Li, S. H. Yu, *Adv. Mater.*, 2013, **25**, 3192.

33 P. Chen, J. J. Yang, S. S. Li, Z. Wang, T. Y. Xiao, Y. H. Qian, S. H. Yu, *Nano Energy*, 2013, **2**, 249.

34 H. L. Peng, Z. Y. Mo, S. J. Liao, H. G. Liang, L. J. Yang, F. Luo, H. Y. Song, Y. L. Zhong, B. Q. Zhang, *Sci Rep-Uk*, 2013, **3**.

35 Q. Wang, Z. Y. Zhou, Y. J. Lai, Y. You, J. G. Liu, X. L. Wu, E. Terefe, C. Chen, L. Song, M. Rauf, N. Tian, S. G. Sun, *J. Am. Chem. Soc.*, 2014, **136**, 10882.

36 Y. Y. Liang, H. L. Wang, P. Diao, W. Chang, G. S. Hong, Y. G. Li, M. Gong, L. M. Xie, J. G. Zhou, J. Wang, T. Z. Regier, F. Wei, H. J. Dai, *J. Am. Chem. Soc.*, 2012, **134**, 15849.

37 X. J. Huang, Y. G. Tang, L. F. Yang, P. Chen, Q. S. Wu, Z. Pan, J. Mater. Chem. A, 2015, 3, 2978.

38 H. B. Lu, W. M. Huang, Appl. Phys. Lett. 2013, 102, 231910

39 H. B. Lu, Y. T. Yao, W. M. Huang, D. Hui, Compos. Part B-Eng. 2014, **67**, 290.

N-, Fe- and Co-tridoped carbon nanotube/nanoporous carbon nanocomposite from Typha orientalis was prepared and the typical product exhibits the excellent ORR activity in acidic media.